Measuring Concrete Crosstie Rail Seat Pressure Distribution

with Matrix Based Tactile Surface Sensors

AREMA 2012 Annual Conference
September 16-19, 2012

Christopher T. Rapp[1], Marcus S. Dersch[2], J. Riley Edwards[2], Christopher P. L. Barkan[2],
Brent Wilson[3], and Jose Mediavilla[4]

Rail Transportation and Engineering Center – RailTEC [2]
Department of Civil and Environmental Engineering
University of Illinois at Urbana-Champaign
205 N. Mathews Ave., Urbana, IL 61801

Amsted Rail [3]
1700 Walnut St.
Granite City, IL 62040

Amsted RPS [4]
8400 W. 110th St, Ste 300
Overland Park, KS 66210

6,679 Words, 4 Tables, 10 Figures

Christopher T. Rapp	Marcus S. Dersch	J. Riley Edwards
(513) 406-1520	(217) 333-6232	(217) 244-7417
ctrapp3@illinois.edu	mdersch2@illinois.edu	jedward2@illinois.edu

Christopher P.L. Barkan	Jose Mediavilla	Brent Wilson
(217) 244-6338	(913) 345-4807	(618) 451-8201
cbarkan@illinois.edu	jose@amstedrps.com	bwilson@amstedrail.com

[1] Corresponding author

ABSTRACT

A sustained increase in gross rail loads and cumulative freight tonnages, as well as increased interest in high speed passenger rail development, is placing an increasing demand on North American railway infrastructure and its components. To meet this demand, concrete crossties will require increased strength and durability, and the industry must also develop a deeper understanding of failure modes. One of the typical failure modes for concrete crossties in North America is Rail Seat Deterioration (RSD), which can initiate through multiple failure mechanisms. Researchers have hypothesized that localized crushing of the concrete in the rail seat is one of the potential mechanisms that contributes to RSD. To better understand this mechanism, the University of Illinois at Urbana-Champaign (UIUC) is utilizing a matrix based tactile surface sensor (MBTSS) to measure and quantify the forces and pressure distribution acting at the contact interface between the concrete rail seat and the bottom of the rail pad. Preliminary data collected during laboratory testing has shown that a direct relationship exists between rail pad modulus (stiffness) and maximum rail seat force. A direct relationship between the lateral/vertical (L/V) force ratio and the maximum field side rail seat force has also been observed. Given that all preliminary results indicate that various combinations of pad stiffness, track geometry, and L/V ratios create localized areas of high pressure, crushing remains a potential mechanism leading to RSD, as will be discussed in this paper. Through the analysis of rail seat pressure data, valuable insight will be gained that can be applied to the development of concrete crosstie and fastening system component designs that meet current and projected service demands.

INTRODUCTION

Concrete crossties are most economical in locations that place high demands on the railroad track structure and/or necessitate stringent geometric tolerances. For North American use, they were adopted in response to the inability of timber crossties to perform satisfactorily in certain severe service conditions, such as areas of high curvature, heavy axle load or high speed passenger train traffic, high annual gross tonnages, steep grades, and severe climatic conditions *(1).* The cast-in shoulders and molded rail seat of concrete crossties increase their ability to hold gage under these loading conditions *(1).*

Concrete crossties are not without their design and performance challenges. As reported in surveys conducted by the University of Illinois at Urbana-Champaign (UIUC) in 2008 and 2012, North American Class I Railroads and other railway infrastructure experts ranked rail seat deterioration (RSD) as one of the most critical problems associated with concrete crosstie and fastening system performance *(2, 3).* Problems that arise from the deterioration of the concrete rail seat surface include widening of gauge, reduction in toe load of fastening clips, and insufficient rail cant *(2).* All of these problems have the potential to create unsafe operating conditions and an increased risk of rail rollover derailments *(4).*

A suspected cause of RSD is high forces acting on the concrete rail seat surface, often in concentrated areas. To address this, a study was performed by the John A. Volpe National Transportation Systems Center on the effect of wheel/rail loads on concrete tie stresses and rail rollover. This study confirmed the possibility of these concentrated loadings producing stresses higher than the minimum design compressive strength of concrete as specified by the American Railway Engineering and Maintenance-of-Way Association (AREMA) *(4).*

The combination of static wheel loads and the dynamic impact loads that can occur due to track support variations, wheel defects, or rail irregularities, impart loads into the rail seat that potentially damage the concrete surface *(5)*. In North America, concrete crosstie track is often much stiffer than timber track. According to the *AREMA Manual for Railway Engineering,* the typical track modulus value for mainline concrete crosstie track is 6,000 lb/in^2, which is twice as stiff as the typical timber crosstie track modulus of 3,000 lb/in^2 *(6)*. A track structure that is stiffer produces a less resilient response to impact loads, resulting in higher loads being applied to the concrete rail seat surface.

To better understand the forces acting at this surface, researchers at UIUC are using matrix based tactile surface sensors (MBTSS) as a means to measure load magnitude and distribution. MBTSS have been previously used in experimentation under the tie plates on timber crossties *(7);* however, researchers at UIUC are using this technology to explore the pressure distribution on the rail seats of concrete crossties.

There are many factors that affect the rail seat pressure distribution, one of which is the transfer of forces at the wheel/rail interface. As the load is transferred from the wheel to the rail, it moves through the web of the rail and into the base of the rail. Next, the load is distributed through the rail pad assembly onto the rail seat of the crosstie. The profile of the wheel and rail (e.g. wear pattern), and the performance of the rail car truck, govern the location and angle of the resultant force. The authors of this paper suspect that these parameters can cause significant variation in what areas of the rail seat are receiving concentrated loadings. Additionally, the lateral to vertical (L/V) ratio of this resultant force also varies greatly depending on track geometry conditions. Horizontal curvature can greatly increase the lateral forces due to flanging forces of wheels. Trains travelling at speeds above or below the balancing speed of a curve can cause shifts in the vertical and lateral load to the high or low rail, respectively. These loading scenarios are especially likely on shared infrastructure, where both freight and

passenger trains run on the same track, typically at different speeds. Shared infrastructure presents diverging engineering requirements for track that can accommodate the heavy axle loads of slower speed freight trains with the possibility of high dynamic loads from higher speed passenger trains.

Design of the fastening system components also plays a crucial role in the distribution of pressure in the rail seat. Given the stiff nature of concrete crosstie track, the fastening system must provide some of the resiliency necessary to attenuate loads without damaging the concrete *(8)*. The variables potentially affecting the magnitude and distribution of pressure on concrete rail seat are explored through laboratory experimentation. Preliminary results from these experimental tests are documented in this paper.

SENSOR TECHNOLOGY AND PROTECTION

The sensor technology UIUC is currently using for quantifying forces and pressure distribution at the rail seat is the MBTSS manufactured by Tekscan® Inc. The MBTSS is comprised of two thin sheets of polyester with a total thickness of 0.004 inches (0.01 cm) (Figure 1). On one of the sheets, a pressure sensitive semi-conductive material is printed in rows. On the other sheet, the same semi-conductive material is printed in columns, which form a grid when the two sheets are overlaid. Conductive silver leads extend from each column and row to the area of the sensor from which data is collected. Glue is applied around the edges so as to bond the two sheets together and avoid the intrusion of foreign materials or moisture into the pressure sensing area.
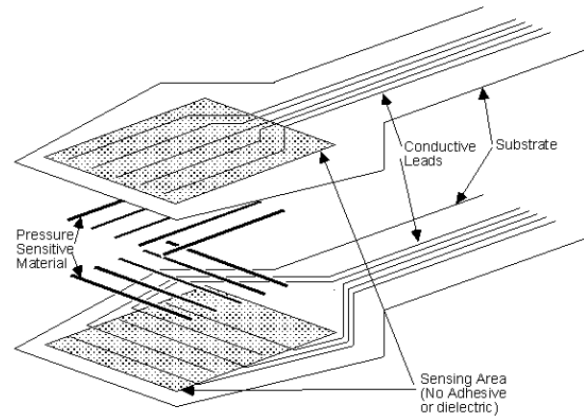
FIGURE 1. Exploded View of a Tekscan® Sensor *(7)*

The behavior of these sensors is similar to that of a resistive transducer (e.g. strain gauge). As a force is applied to the pressure sensitive area, the resistivity in the overlain circuits changes and the output is collected by the Data Acquisition Handle (DAH). The DAH connects the sensor to a computer via a Universal Serial Bus (USB) cable. The intersection of each printed row and column creates a sensing location, which represents one cell of data output to the computer software. The number of sensing locations is dependent upon the number of rows and columns in the matrix. For example, the Tekscan® sensor model/map 5250, which is currently being used by UIUC researchers, is comprised of 44 rows and 44 columns, creating 1,936 pressure sensing locations *(9)*. For this model, each row and column has a width of 0.22 inches (0.56 cm), thus each sensing location has an area of 0.0484 in^2 (0.31 cm^2) *(9)*. This creates a resolution of approximately 21 sensing locations per square inch (3.23 per cm^2). The computer software is able to output the contact area of an imparted load by multiplying the number of sensing locations receiving force by the area of each.

The concrete rail seat can be a coarse and uneven surface, often due to the steel forms and other aspects of the concrete crosstie manufacturing process. Abrasive fines consisting of cement particles and aggregate from the deteriorated concrete surface,

sand or other fines from the surrounding environment, and metal filings from the rail or cast-in steel shoulders are often present - even in well-maintained track. Given the sensor's susceptibility to being punctured or damaged by irregular surfaces, it is important to provide protection for the sensing surface. Any puncture or physical interference to the sensor can cause permanent damage and erroneous data collection. Furthermore, because loads are rarely applied purely perpendicular (vertical) to the rail seat, there can also be shear forces at this interface due to the influence of lateral loads. To protect from puncture damage, a thin layer of bi-axially oriented Polyethylene Terephthalate (BoPET) is placed on each side of the sensor when installed on a rail seat (Figure 2), and to protect the sensor from shear forces, a thin sheet of polytetrafluoroethylene (PTFE) is also layered on either side between the sensor and the BoPET (Figure 2). PTFE's low coefficient of friction makes it an appropriate choice to mitigate excessive lateral loads or frictional forces from longitudinal stress in the rail.
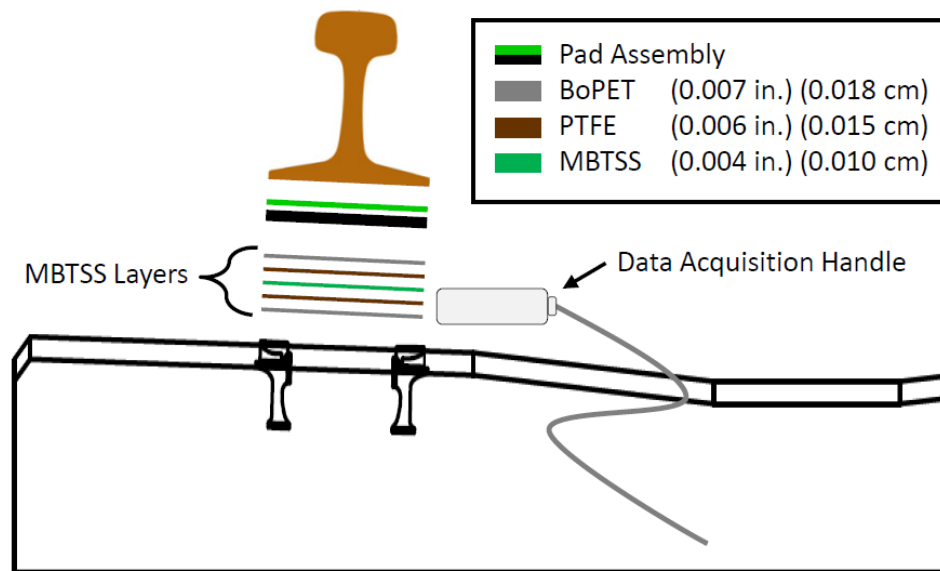
FIGURE 2. Profile View of MBTSS Layers and Thicknesses

DATA ACQUISITION

The data are not initially output in a unit of force, but rather as a "raw sum unit". The sensors, having an 8-bit output, measure force on a scale of 0-255, with a value of 255 indicating that a sensor is fully saturated at that location and cannot measure additional increases in load. To obtain useable engineering units from the raw sum units, a calibration file must be applied. Calibration of MBTSS is conducted by applying known loads and correlating the loads with the respective raw sum units. This process emphasizes the importance of laboratory testing and familiarization with the technology prior to performing field testing.

PREVIOUS RAIL SEAT PRESSURE MEASUREMENT INSTRUMENTATION

Previous research has been conducted using the sensors produced by Tekscan® to analyze loads at the tie plate and timber crosstie interface *(7)*. This work was conducted by the University of Kentucky (UK) to develop a non-invasive means to measure the forces and pressures imparted into the timber crosstie *(7)*. UK researchers first experimented with calibration tests in laboratory settings, and then performed initial field tests on timber crossties.

It was determined from field data that there was an uneven distribution of pressure given the rigid surfaces interacting at this interface. Moreover, there were several high contact points present that bore most of the load. It was also determined that the sensors needed protection from puncture and shear forces, as discussed previously in this paper. Tests to evaluate the variability of plate material on pressure distribution were then performed, using machined steel, polyurethane, rubber pads, and plates *(7)*. From these tests it was concluded that machined steel plates continued to create points of peak pressure, whereas the presence of a softer material at this interface, such as

rubber or polyurethane plastic, increases contact area resulting in more evenly distributed forces and lower contact pressures.

UK's research confirmed the feasibility of using MBTSS to measure pressures at the timber tie rail seat surface in both the laboratory and the field. However, since the research was conducted solely on timber crossties, further validation was needed to determine MBTSS' viability for concrete crosstie rail seat pressure measurement. Researchers at UIUC are expanding the use of this technology to analyze the loads imparted on the concrete rail seats, and to provide future design recommendations to mitigate performance problems such as RSD.

EXPERIMENTAL SETUP

UIUC's experimental testing was performed at the Advanced Transportation Research and Engineering Laboratory (ATREL). The Pulsating Load Testing Machine (PLTM), which is used to perform American Railway Engineering and Maintenance-of-way Association (AREMA) Test 6 (Wear and Abrasion), as well as other experimental testing related to concrete crossties and fastening systems, was used to execute the experiments within this paper. The loading conditions for AREMA Test 6 are meant to simulate heavy-haul severe-service conditions, such as those experienced on horizontal curves greater than five degrees *(6).* The PLTM consists of one horizontal and two vertical actuators, both attached to a steel loading head that encapsulates a short section of rail attached to one of the two rail seats on a concrete crosstie. This actuator arrangement allows for the L/V ratio to be varied without changing the physical arrangement of the actuators, loading frame, or concrete crosstie. Furthermore, by using MTS MultiPurpose TestWare® (MPT), a wide variety of test procedures can be designed in an attempt to simulate various field conditions.

Preliminary UIUC research included installing a MBTSS in the concrete crosstie fastening system and loading the tie using the PLTM (Figure 3). The same MBTSS was used throughout each respective experiment to remove the possibility of inter-sensor variability.

**FIGURE 3. MBTSS Instrumentation at UIUC**

RESULTS OF EXPERIMENTATION

Several experiments have been conducted by UIUC researchers to collect data on the distribution of pressure on the concrete crosstie rail seat based on expected loading conditions at the rail seat. It should be noted that the experimental setup is not meant to replicate the common loading conditions seen in the field, but is designed to simulate extreme loading conditions that occur in the field. Therefore, this experimental setup simulates a single wheel load imparted onto a single crosstie.

These tests were conducted to analyze and quantify the loading behavior at this interface using a variety of load inputs while varying concrete crosstie fastening system components. The first series of tests was performed to determine a relationship between the rail pad modulus (a proxy for stiffness) and pressure distribution at the rail seat. Another series of tests was performed to compare two different fastening system clip designs with respect to their ability to distribute pressure over the rail seat. For each

series of tests, various L/V ratios were explored in an attempt to simulate a variety of rail vehicle and track interaction conditions that could occur at the wheel/rail interface. The overall objective of this testing was to determine a relationship between L/V ratio and pressure distribution at the rail seat varying different components of the fastening system. The following sections explain the effect of varying L/V ratios, and present the testing protocol and results from the aforementioned experiments.

LATERAL TO VERTICAL (L/V) LOAD RATIOS

It is possible that the distribution of pressure is affected by the location and angle of the resultant force that transfers the load from the wheel to the head of the rail. The angle of the resultant force can vary greatly based on both the wear conditions of the rail and the wheels. This resultant force can be broken into lateral and vertical components to allow for a more detailed analysis of the wheel/rail interface (Figure 4).

Resultant Force of Wheel Load   L/V Components of Resultant Force
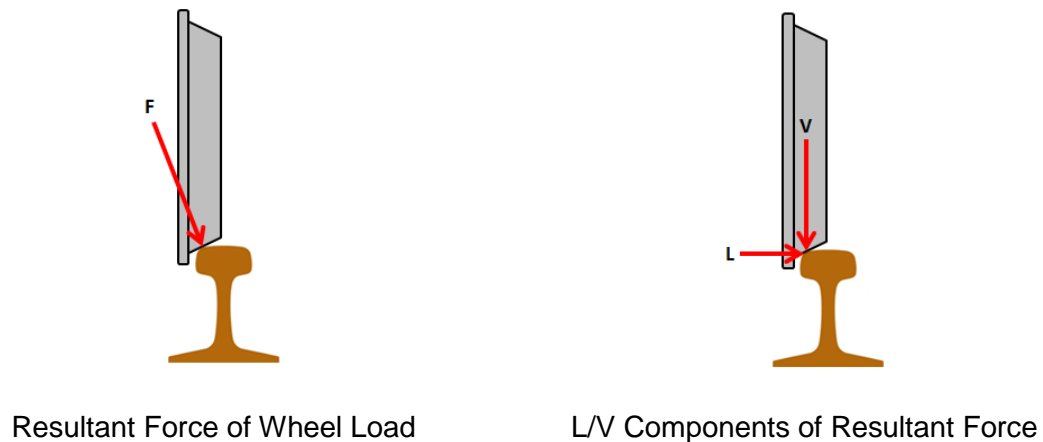
FIGURE 4. Forces at Wheel/Rail Interface

There are many variables that can affect the L/V ratio, including the curve radius, wheel/rail interface profiles, suspension characteristics of railcar trucks, and train speed *(10).* On curved track, it is common for trains to operate at speeds other than the balancing speed. Freight trains may operate below the balancing speed for a particular

curve, shifting the highest loads toward the inside of the curve. This is known as an overbalanced condition, where the center of mass of each car is inside of the equilibrium point, causing the car to lean towards the low rail. In this scenario, the low rail seat of a crosstie will be experiencing a much higher load than the high rail seat due to the shift of the vertical load *(11)*. Also, if a train is operating in an underbalanced condition, where the center of mass of each car is outside of the equilibrium point, loads will not be evenly distributed, and will concentrate on the field side.

Researchers at UIUC are also studying the possibility that a high L/V ratio places an excessive amount of strain on the fastening system components. This could greatly affect the system's structural integrity and its ability to remain an elastic, load-absorbing element in the relatively stiff concrete crosstie track. Furthermore, a high L/V ratio increases the risk of rail rollover conditions, which can lead to a derailment *(10)*. To gain a better understanding of the distribution of pressure at this interface, various L/V ratios were input into the MPT program to perform the rail pad and clip tests. Through this testing, the effect of pad modulus and clip type on pressure distribution can be analyzed, as can the effect of varying the L/V ratio. Since the L/V ratio of 0.52 is the standard used in AREMA Test 6 to simulate severe service conditions, it was chosen as one of the values to test *(6)*.

For the series of tests performed on the two clip types, two lower L/V values of 0.25 and 0.44 were chosen to simulate curvature of a lower degree and possibly a tangent track condition. A higher value of 0.60 was also chosen to collect data for a more extreme condition with very high lateral forces. The series of pad modulus tests were performed at a later date than the clip tests, and it was decided to include the L/V ratios of 0.48 and 0.56 into the testing procedure for the purpose of collecting more data points that are linearly spaced.

It can be seen from the results presented in the following sections that a higher L/V ratio results in a lower rail seat contact areas for pressure distribution. Additionally, the contact area tends to be concentrated towards the field side of each rail seat. As an example, between the L/V ratios of 0.25 and 0.60 for a Thermoplastic Vulcanizate (TPV) rail pad, the area of the rail seat being loaded is reduced by 7.45 in^2 (48.06 cm^2), resulting in peak pressures that are approximately 1,300 psi (8.96 mPa) higher (Table 2). This trend reading increasing L/V ratios can be seen for all series of tests that were performed.

Researchers at UIUC theorize that this high concentration of field side loading could be seen on the high rail seat on a section of superelevated track with a train operating in an underbalanced condition. Inversely, a field side concentration on the low rail seat would be expected for a train operating in an overbalanced condition.   This is also based on the field observations from sections of track with varying types of concrete crossties and fastening systems, as well environmental conditions, where more deterioration has occurred on the field side of rail seats - especially on curves. In these observations it was assumed that the various concrete crossties were designed to meet similar specifications and thus would have similar strength and design characteristics, allowing for a qualitative comparison between the locations.

The study performed by researchers at the John A. Volpe National Transportation Systems Center supports this possibility of concentrated field side loadings in presenting a theoretical triangular loading pattern based off of the L/V ratio, width of the rail base, and eccentricity of the loading conditions *(4)*. These researchers also noted this larger magnitude of deterioration occurring on the field side in their investigation of two rail rollover scenarios which resulted in derailments *(4)*.

RAIL PAD MODULUS TEST

Concrete crosstie fastening systems typically include a single or multi-layer rail pad assembly *(12).* Part of this assembly includes a rubber or polyethylene rail pad to attenuate the load and provide protection for the concrete rail seat *(1).* When viewed as a single structural element consisting of the subballast, ballast, concrete crosstie, fastening system, and rail, concrete crosstie track in North America is often more rigid than the traditional timber crosstie track. Because of this, concrete crossties can impart higher stresses onto the ballast layer under train loading. An important purpose of the rail pad as an individual component is to provide increased resiliency for the concrete crosstie system. The increased resiliency provides the advantages of increased comfort for passengers and protection of the rolling stock *(13).* Rail pads are manufactured from a variety of materials and molded into different geometries, which in turn govern the rail pad modulus. Rail pad modulus is a value that defines the stiffness of the material.

Part of the research being conducted at UIUC is investigating the effect of the rail pad's modulus (stiffness) on mitigating high loads imparted on the rail seat while continuing to protect the concrete rail seat. Researchers at UIUC are exploring the possibility that a rail pad of a lower modulus (i.e. softer) will distribute the applied load over a wider area of the concrete rail seat. Although a softer rail pad may better mitigate high impact loads, its high resiliency allows for greater rail deflection, which can increase wear and fatigue of other components of the fastening system *(1).* The softer pad in combination with the elastic clips commonly used in concrete crosstie fastening systems can perform well in moderate traffic loading conditions, but under heavier loads as are becoming increasingly common in North America, excessive lateral movement and wear can occur *(12).*

In performing the AREMA Test 6 (Wear and Abrasion) using the PLTM, researchers at UIUC have seen this excessive lateral movement of the rail cause wear on the field

side cast-in steel shoulder, which could potentially lead to gauge-widening. In both the 2008 and 2012 surveys of North American Class I Railroads, shoulder/fastener wear or fatigue ranked second behind RSD as the second most critical concrete tie problem *(2, 3)*. Also, UIUC researchers are exploring the possibility that a rail pad with higher modulus (i.e. stiffer) will help reduce the stress on the fastening system as a whole, but will place a higher concentration of load on the concrete rail seat surface, and in turn result in increased ballast pressures on the bottom of the crosstie *(12)*.

An experiment was performed to compare the pressure distribution of a higher modulus, medium density polyethylene (MDPE) rail pad to a low modulus Thermoplastic Vulcanizate (TPV) rail pad. The rail pads used were cast with a flat surface specifically for this experiment to remove variation in pad geometry. Table 1 shows both the TPV and MDPE pads used for this experiment.   It should be noted that although the numerical value for the TPV rail pad Shore Hardness is higher than that of the MDPE, the type A scale is used for softer plastic materials, whereas the type D is used for harder plastic materials. In this instance, the value of 60 for the type D scale indicates a harder material than does the value of 86 for the type A scale.

TABLE 1. Components and Material Properties for Rail Pad Test

	TPV	MDPE
Shore Hardness and Scale	86 (A)	60 (D)
Flexural Modulus, psi (mPa)	15,000* (103.42)	120,000 (827.37)

*Approximate flexural modulus based on a TPV with a similar Shore Hardness of 87A

Loading conditions were consistent for both series of tests, having a constant vertical load of 32,500 lb (144.56 kN) and corresponding lateral loads based on the L/V ratios being simulated.   To compare the relative performances of the two rail pads, the maximum loaded frame per L/V ratio was identified and obtained for each pad (Figure 5). Table 2 is a compilation of the results from this series of tests. The data collected for each rail pad is presented side-by-side by L/V ratio to show the difference in pressure distribution for the two materials under identical loading conditions. Figure 6 is a plot of the average pressure per column of data from the MBTSS along the width of the rail seat for the TPV rail pad, by L/V ratio. Figure 7 is the same plot of data collected during the MDPE rail pad test.
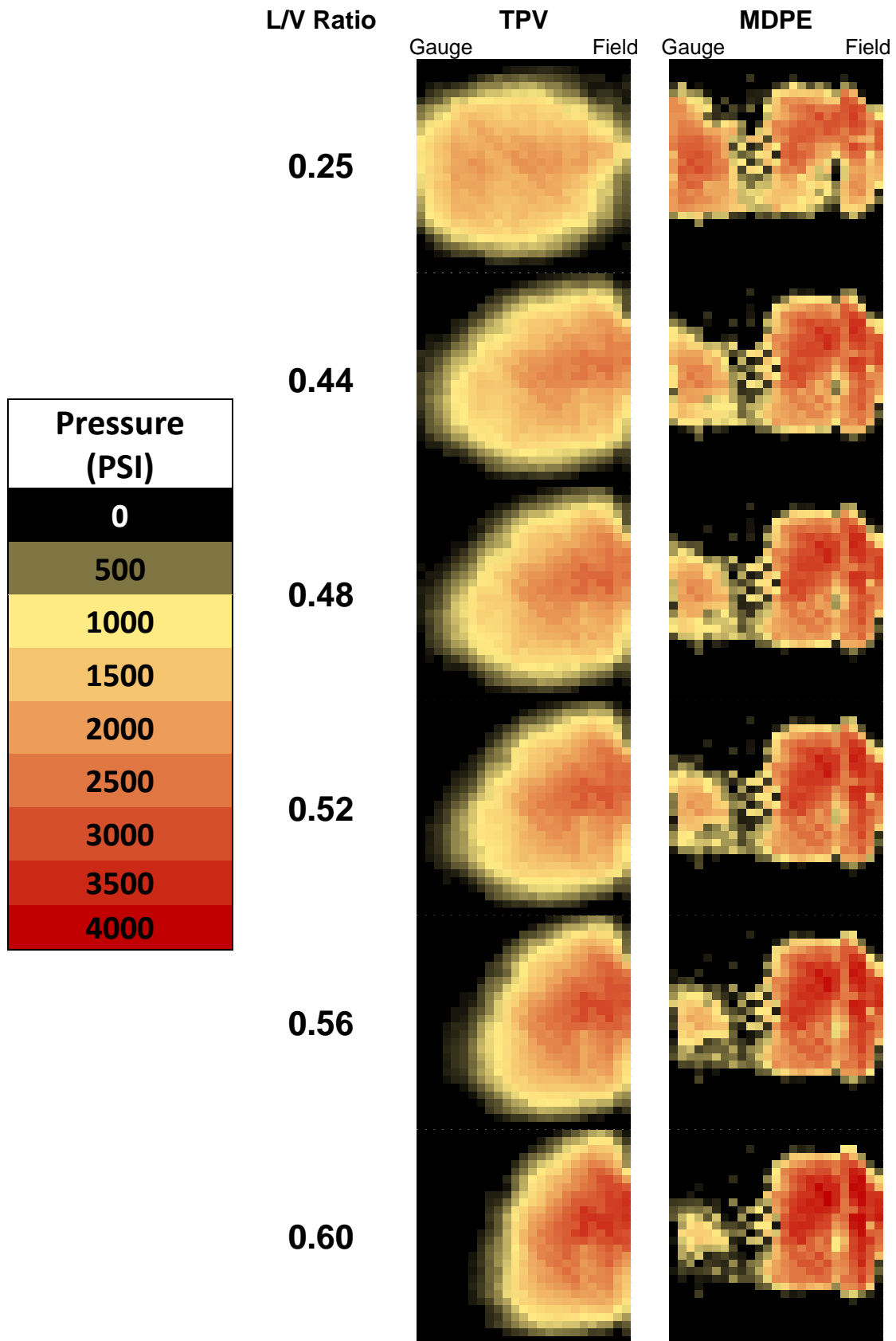
FIGURE 5. Comparison of Rail Seat Pressure Distributions for Different Pad Moduli and Varying L/V Ratios

TABLE 2. Results of Rail Pad Modulus Test

L/V Ratio	0.25		0.44		0.48	
Pad Material	MDPE	TPV	MDPE	TPV	MDPE	TPV
Vertical, kips (kN)	32.50 (144.56)	32.50 (144.56)	32.50 (144.56)	32.50 (144.56)	32.50 (144.56)	32.50 (144.56)
Lateral, kips (kN)	8.13 (36.14)	8.13 (36.14)	14.30 (63.61)	14.30 (63.61)	15.60 (69.39)	15.60 (69.39)
Contact Area, in^2 (cm^2)	20.09 (129.61)	28.75 (185.48)	19.31 (124.58)	27.93 (180.19)	19.12 (123.35)	27.25 (175.81)
% of Rail Seat	59	85	57	82	56	80
Peak Pressure, psi (mPa)	3,213 (22.15)	2,139 (14.75)	3,469 (23.92)	2,573 (17.74)	3,546 (24.45)	2,800 (19.31)
Contact Area over 3000 psi, in^2 (cm^2)	0.34 (2.19)	0	1.55 (10.00)	0	2.32 (14.97)	0

| L/V Ratio	0.52		0.56		0.60	
Pad Material	MDPE	TPV	MDPE	TPV	MDPE	TPV
Vertical, kips (kN)	32.50 (144.56)	32.50 (144.56)	32.50 (144.56)	32.50 (144.56)	32.50 (144.56)	32.50 (144.56)
Lateral, kips (kN)	16.90 (75.17)	16.90 (75.17)	18.20 (80.96)	18.20 (80.96)	19.50 (86.74)	19.50 (86.74)
Contact Area, in^2 (cm^2)	19.02 (122.71)	25.75 (166.13)	18.63 (120.19)	23.96 (154.58)	17.76 (114.58)	21.30 (137.42)
% of Rail Seat	56	76	55	71	52	63
Peak Pressure, psi (mPa)	3,721 (25.66)	2,925 (20.17)	3,838 (26.46)	3,162 (21.80)	4,096 (28.24)	3,400 (23.44)
Contact Area over 3000 psi, in^2 (cm^2)	2.86 (18.45)	0	3.44 (22.19)	0.53 (3.42)	4.11 (26.52)	1.74 (11.23)
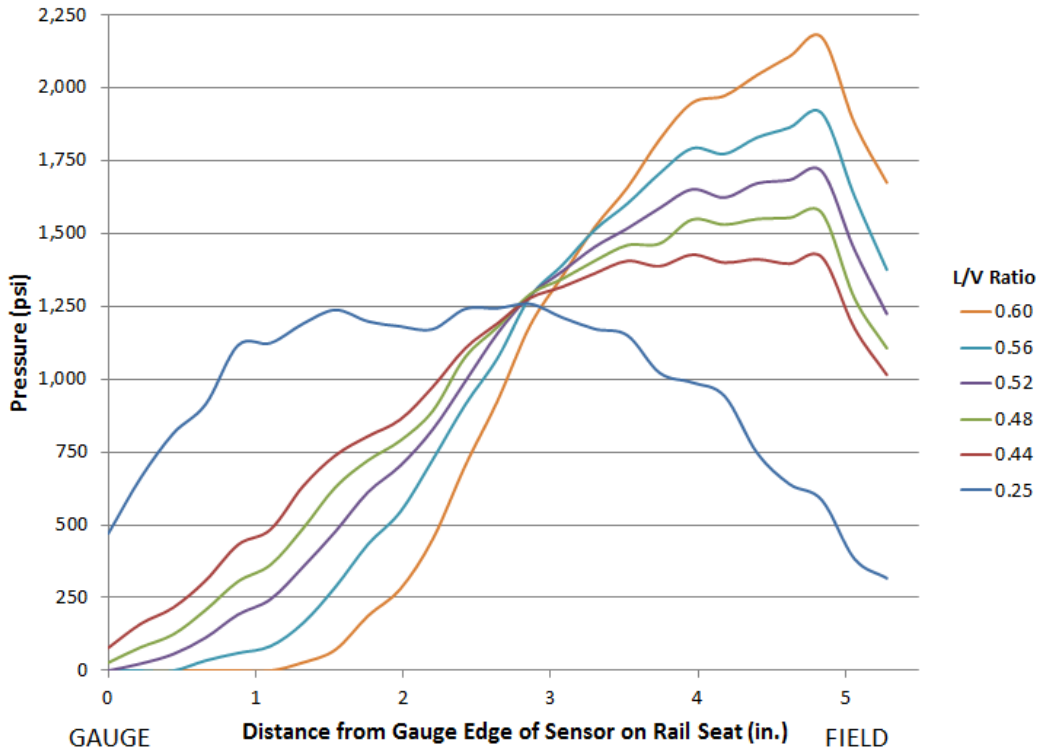
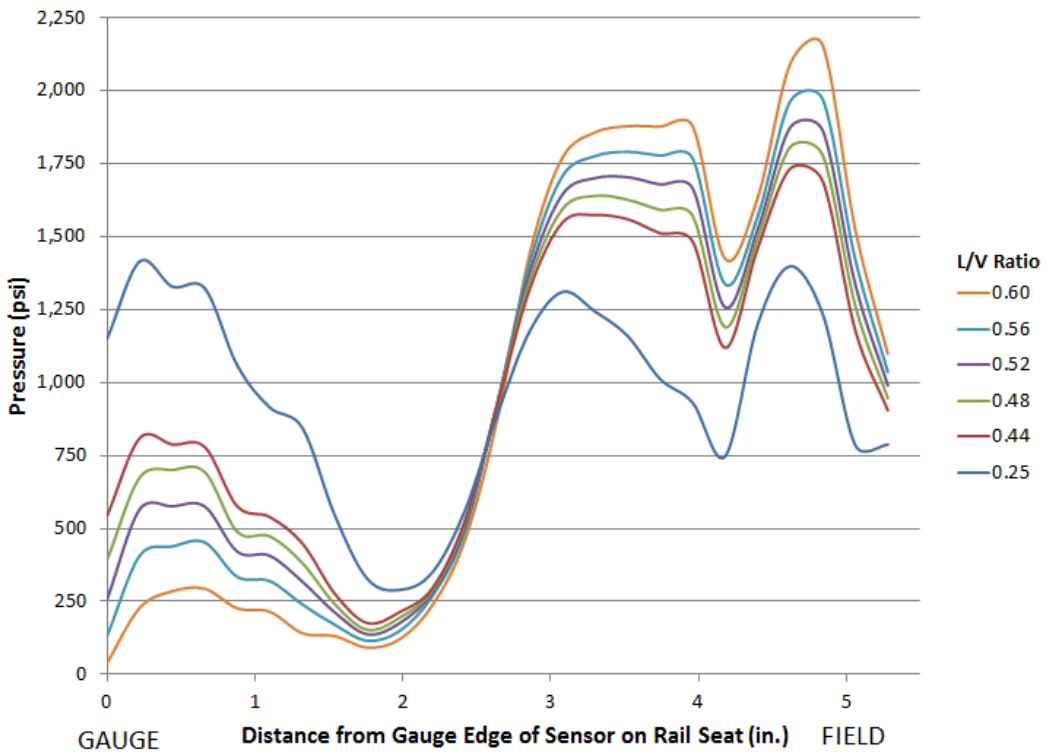**FIGURE 6. Average Pressure Distribution for TPV Rail Pad**

FIGURE 7. Average Pressure Distribution for MDPE Rail Pad

This experiment shows that the MDPE rail pad distributed the same applied load over a noticeably smaller area of the rail seat than the low modulus TPV rail pad. For an L/V ratio of 0.25, the contact area of the load for the high modulus MDPE rail pad was 20.09 in^2 (129.61 cm^2), which is only 70% of the 28.75 in^2 (185.48 cm^2) of contact area recorded for the low modulus TPV rail pad under the same load. This reduced the total percentage of rail seat area being loaded from approximately 85% to 59%. Peak pressures for each pad occurred during the L/V ratio of 0.60, as it was the same vertical load being applied to smaller areas. For the MDPE rail pad, this value was 4,096 psi (28.24 mPa); approximately 20% higher than the 3,400 psi (23.44 mPa) recorded for the TPV rail pad, and it distributed the load over 11% less of the rail seat surface. It should also be noted that although the MDPE rail pad had a smaller total contact area, it had a larger amount of area loaded at higher pressures, as is evident in the rows showing contact area over 3,000 psi (20.68 mPa) (Table 2).

In Figures 6 and 7, the increase of loading into the field side of the rail seat as L/V ratio increases can be seen for both pad materials. In both instances, the decrease of pressure in the area immediately adjacent to the field side shoulder is likely due to the gap beneath the insulator post beyond the width of the base of the rail. The shape of the curves for each test could be due to variable material geometry or properties, which can in turn govern the rail base rotation, of each rail pad material under increasing L/V ratios. Additional test replicates are needed to gain additional insight on the shape of the curve on an average rail seat. The curves for the TPV pad are similar to the theoretical triangular distribution pattern noted in previous concrete crosstie rail seat stress research *(4).* This could be due to the fact that the lower stiffness of the TPV pad allows the base of the rail to rotate greater under increased lateral loads. The stiffer MDPE pad, however. would allow less rotation of the rail base, resulting in the distributions shown in Figure 7.

It should be noted that for this test, and the following clip component test, data was not collected in the area immediately adjacent to the gauge side of the rail seat (as can be seen on the gauge side of the plotted areas for Figures 6 and 7). This is due to the need to protect the MBTSS by allowing the silver conductive leads extending from the pressure sensitive area of the sensor to lay flat on the rail seat, rather than bending that area over the base of the rail. Bending of the sensor around the base of the rail was found to cause damage to the sensor in earlier experimentation. Sacrificing this small amount of data collection on the gauge side was accepted by the researchers at UIUC, as the pressures near the field side are the primary target of investigation.

From this experiment, it can be seen that a direct relationship exists between a high rail pad modulus and concentrated loading of the rail seat. It is also important to note that a highly concentrated loading of the rail seat could lead to crushing of the concrete surface; although the peak pressure values recorded in this laboratory experimentation did not approach the AREMA recommended minimum 28-day-design compressive strength of concrete used for concrete ties of 7,000 psi (48.26 mPa) *(6)*. This is the value that researchers from the John A. Volpe National Transportation Systems Center have been using to compare rail seat pressures calculated from eccentric lateral and vertical wheel/rail loads. These researchers have found that 7,000 psi (48.26 mPa) contact pressures can be exceeded in extreme loading scenarios *(4)*. It is also possible that highly concentrated loads could be seen in the field because although the maximum vertical load explored in this laboratory experimentation was only 32.5 kips (144.56 kN), wheel impact load detector (WILD) sites in revenue service can record loads of greater than 100 kips (444.82 kN) *(14)*. It is likely that a load of this magnitude would produce pressures on the rail seat well in excess of 7,000 psi (48.26 mPa).
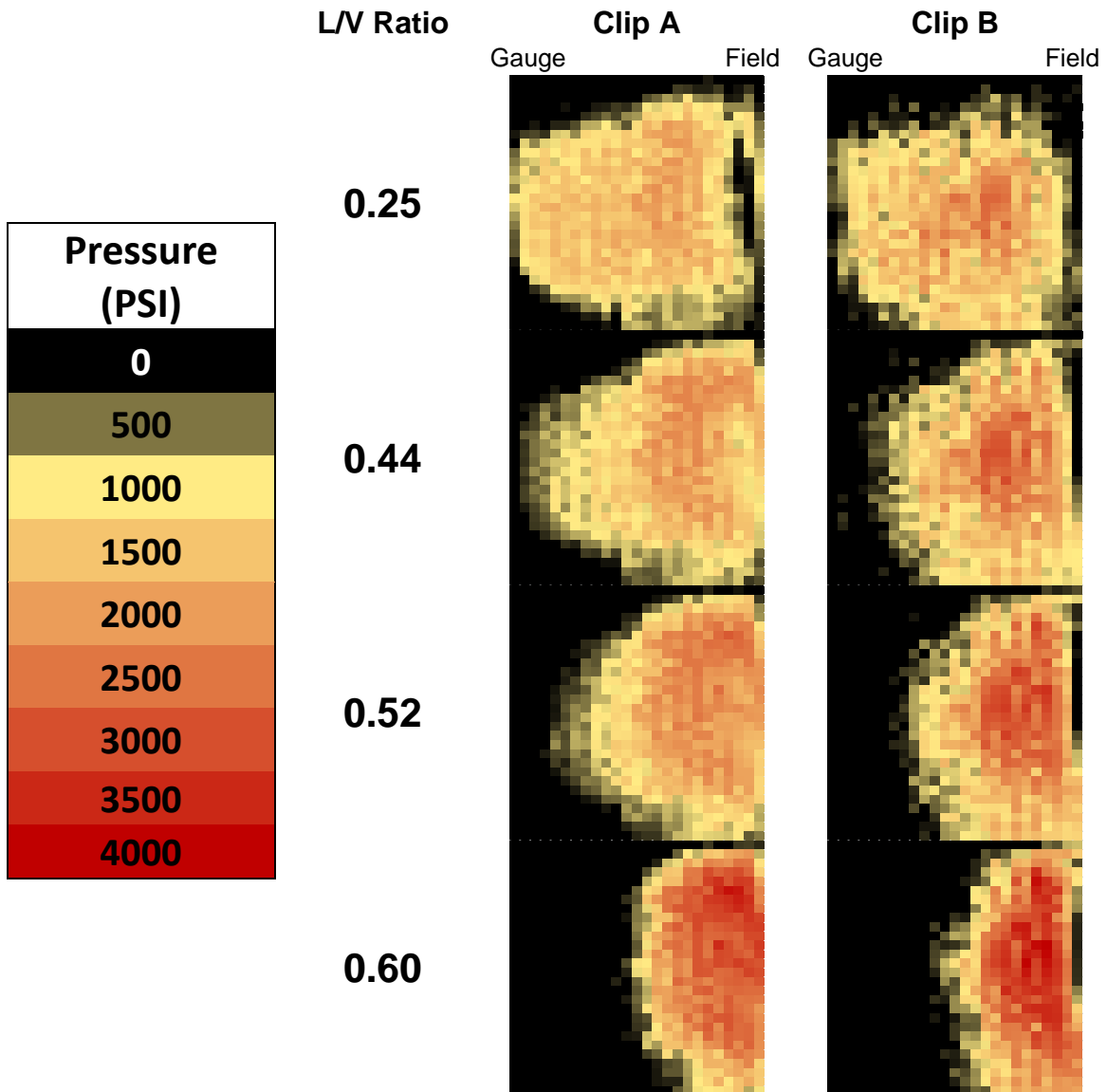
FASTENING CLIP TEST

Fastening systems for concrete crossties serve the primary purposes of providing vertical, lateral, and longitudinal restraint of the rail and providing load attenuation. Various permutations of clip designs and rail pad materials result in concrete track systems with unique stiffness characteristics, which can have a variety of performance consequences on the components, crossties, and ballast (12).

A test was performed to investigate pressure distribution on the rail seat while varying the clip of a concrete crosstie fastening system. Two commonly used fastening system clip designs were used for this test, which will be referred to as Clip A and Clip B (Table 3). The same rail pad assembly was used for each clip to hold that variable constant. It should be noted that a different concrete crosstie had to be used for each respective clip test, as the cast-in steel shoulder design for each fastening system was different (a requirement of different fastening systems). This could result in variability in pressure distributions due to minor differences in the concrete rail seat profile, however no large visual difference was noted between the two crossties used.

TABLE 3. Components and Properties for Fastening Clip Test

	Clip A	Clip B
Toe Load, lbs (kN)	4,750 (21.13)	5,500 (24.47)
Spring Rate, lb/in (kN/mm)	8,223 (1.44)	6,286 (1.10)

Loading conditions were consistent for both series of tests, having a constant vertical load of 32,500 lb (144.56 kN) and corresponding lateral loads based on the L/V ratios simulated. Four L/V ratios were used for this test, ranging from 0.25 to 0.60. To compare the relative performances of the two clip designs, the maximum loaded frame per L/V ratio was obtained for each clip (Figure 8). Table 4 is a summary of results from these maximum loaded frames. Figure 9 is a plot of the average pressure per column of data from the MBTSS along the width of the rail seat for Clip A, per L/V ratio. Figure 10 is the same plot of data collected during the test for Clip B.

**FIGURE 8. Comparison of Rail Seat Pressure Distributions for
Two Differing Fastening Clips**

TABLE 4. Results of Fastening Clip Test

L/V Ratio	0.25		0.44		0.52		0.60	
Clip Design	Clip A	Clip B	Clip A	Clip B	Clip A	Clip B	Clip A	Clip B
Vertical, kips (kN)	32.50 (144.56)	32.50 (144.56)	32.50 (144.56)	32.50 (144.56)	32.50 (144.56)	32.50 (144.56)	32.50 (144.56)	32.50 (144.56)
Lateral, kips (kN)	8.13 (36.14)	8.13 (36.14)	14.30 (63.61)	14.30 (63.61)	16.90 (75.17)	16.90 (75.17)	19.50 (86.74)	19.50 (86.74)
Contact Area, in^2 (cm^2)	28.36 (182.97)	27.59 (178.00)	26.57 (171.42)	24.54 (158.32)	23.62 (152.39)	21.01 (135.55)	16.55 (106.77)	17.18 (110.84)
% of Rail Seat	84	81	78	72	70	62	49	51
Peak Pressure, psi (mPa)	2,188 (15.09)	2,744 (18.92)	2,327 (16.04)	3,067 (21.15)	2,872 (19.80)	3,385 (23.34)	3,809 (26.26)	4,083 (28.15)
Contact Area over 3000 psi, in^2 (cm^2)	0	0	0	0.24 (1.55)	0	0.92 (5.94)	2.13 (13.74)	3.53 (22.77)
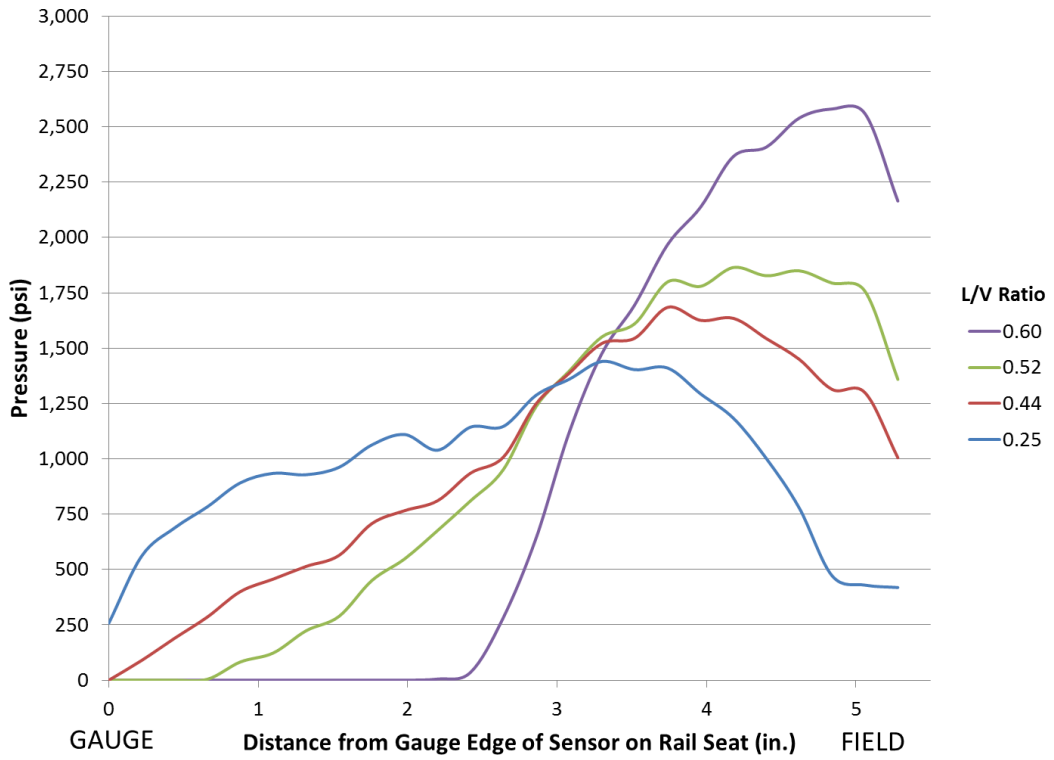
FIGURE 9. Average Pressure Distribution for Clip A

.
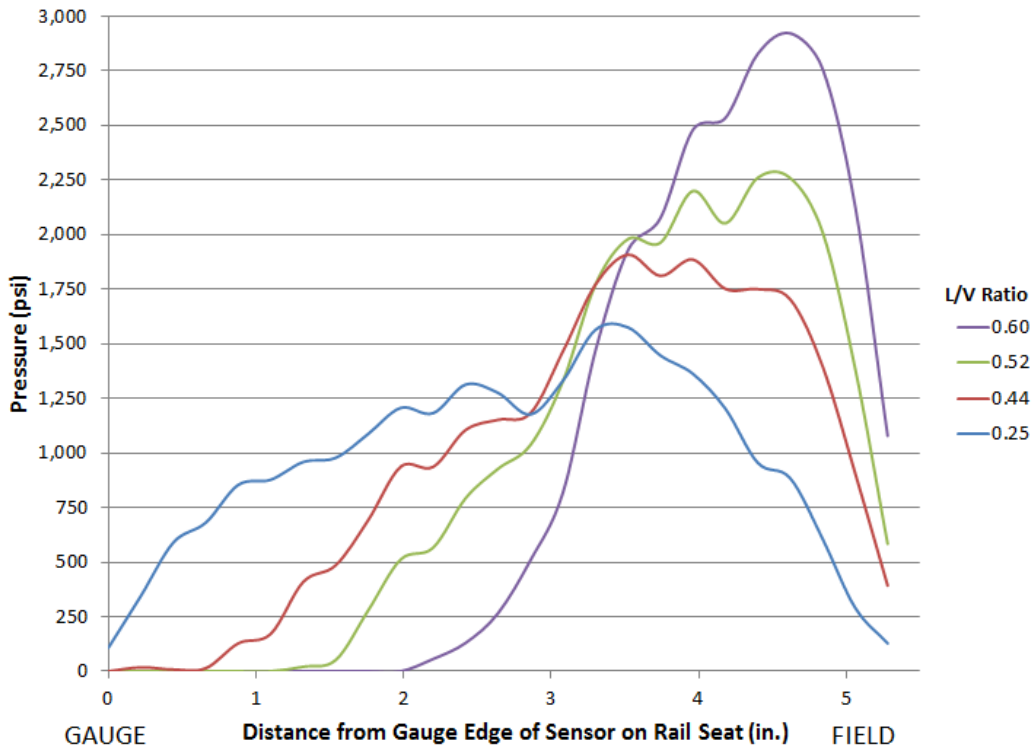
FIGURE 10. Average Pressure Distribution for Clip B

Results from this test show a lower magnitude of variability between these two fastening system components than varying the rail pad material. The general trend was that Clip A clip distributed the pressure over a slightly larger area, thus producing lower peak pressure values. The greatest difference in contact area between the two clips was 2.61 in^2 (16.84 cm^2), at an L/V ratio of 0.52. At the most extreme L/V ratio of the test, the difference in peak pressures was only 274 psi (1.89 mPa), with the value for Clip B being 7.2% higher than that of Clip A.

A notable difference between the results from the two clips is the shapes of the pressure distributions. It appears that the geometry of each clip effects where load is concentrated on the rail seat, but it should be noted that no replicates using additional crossties or fastening systems have been conducted. In all of the pressure distribution frames for Clip B, a central area of concentrated pressure is noted, and the design of this clip is such that there is one point of contact between the clip and in the insulator resting on the rail base, as can be seen in Figure 8. For the Clip A distributions, the peak pressures appear to be concentrated over a wider area of the rail seat, and not concentrated on a single area like Clip B. This appears logical, as design of Clip A has two points of contact between the clip and insulator, as can be seen in Table 3. This concept is also supported by the fact that the Clip B tests showed higher peak pressures being imparted into the rail seat, despite having smaller contact areas than Clip A for all but the L/V ratio of 0.60. Whether these same pressure distributions are seen in the field is not yet known, which we hope to address through future field testing. However, for this laboratory set-up, it is believed that the shape of the pressure distribution is largely a response to the geometry and function of the clip being tested.

CONCLUSIONS AND FUTURE WORK

The following conclusions can be drawn from the analysis of data collected in these preliminary experiments using MBTSS:

- Lower modulus rail pads distribute rail seat loads over a larger contact area, reducing peak pressure values and mitigating highly concentrated loads at this interface

- Higher modulus rail pads distribute rail seat loads in more highly concentrated areas, possibly leading to localized crushing of the concrete surface under extreme loading events

- A lower L/V ratio of the resultant wheel load distributes the pressure over a larger contact area

- A higher L/V ratio of the resultant wheel load causes a concentration of pressure on the field side of the rail seat, resulting in higher peak pressures

- The design of the clip component of the fastening system affects the shape of the pressure distribution on the rail seat

- No large differences in peak pressure or contact area values were seen between the two clip designs tested

Given the projected increase in the use of concrete crossties in the North American railroad industry, research will continue at UIUC to develop a comprehensive laboratory and field instrumentation plan to better understand interactions at this interface. The experiments described in this paper were theoretical in nature, with the loading conditions chosen by researchers based on expert opinion and working knowledge rail seat loads.

Future laboratory testing planned by researchers at UIUC includes installing MBTSS on rail seats of concrete crossties with various models of fastening systems to further

view the effect that variations in clip design have on rail seat pressure distribution. More rail pad modulus testing will take place to better understand the material properties of this component and the effect it has on mitigating rail seat pressures. The pressure distribution for a more commonly used two-part assembly comprising of a Nylon 6-6 abrasion plate and a 95 Shore A TPU pad as compared to the TPV and MDPE pads will also be investigated. Since a load applied to a larger contact area appears to result in lower peak pressure values, testing will also be conducted on crossties with various rail seat dimensions and degrees of deterioration and/or repair via epoxy or other materials. Future testing using more intermediate L/V ratio values will aid the understanding of the transition of pressure from the gauge to field side under an increasing lateral component of the resultant wheel load.

Having run several preliminary tests in the laboratory, as well as developing a means to modify and protect the sensor for more accurate data collection, researchers at UIUC plan to instrument MBTSS on concrete crossties in the field. Field testing will allow analysis of actual loading conditions on the concrete rail seat surface with varying configurations of train loads, speeds, and track geometry.

Field testing will also play a crucial role in guiding the future of laboratory experimentation. A good working relationship between field data and experimental data is expected as the pressure distribution data collection process is refined, and field conditions are better simulated in the laboratory.

In summary, the use of MBTSS appears to be a feasible, non-intrusive means to instrument concrete crossties to measure rail seat pressure distributions. Furthermore, results from this work will be leveraged, as the data collected from MBTSS in the laboratory and field will be used as an input for rail seat loads into finite element model (FEM) analysis of the concrete crosstie and fastening system currently being performed at UIUC.

ACKNOWLEDGEMENTS

REFERENCES

(1)   International Heavy Haul Association. *Guidelines to Best Practices for Heavy Haul Railway Operations, Infrastructure Construction and Maintenance Issues*. D. & F. Scott Publishing, Inc. North Richland Hills, Texas, 2009, Ch. 1,3, and 5, pp. 1-59, 3-67, 3-72, 5-2, and 5-6.

(2)   Zeman, J.C., Chapters 1, 2, and 3, *Hydraulic Mechanisms of Concrete-Tie Rail Seat Deterioration*, M.S. Thesis, University of Illinois at Urbana-Champaign, Urbana, Illinois, 2010, pp. 23 and 29.

(3)   Van Dyk et al 2012.   International Concrete Crosstie and Fastening System Survey – Final Results, University of Illinois at Urbana-Champaign, Results Released June 2012

(4)   Marquis, B.P, Muhlanger, M., Jeong, D.Y., "Effect of Wheel/Rail Loads on Concrete Tie Stresses and Rail Rollover," Proceedings of the ASME 2011 Rail Transportation Division Fall Technical Conference, Minneapolis, MN, September 2011, pp. 1-3.

(5)   Rhodes, D., "How resilient pads protect concrete sleepers," *Railway Gazette International*, February 1988, pp. 85.

(6)   *AREMA Manual for Railway Engineering*, 2009, American Railway Engineering and Maintenance-of-Way Association (AREMA), Landover, Maryland, v 1, Ch. 30.

(7)   Rose, J.G., Stith, J.C., *Pressure Measurements in Railroad Trackbeds at the Rail/Tie Interface using Tekscan Sensors*, University of Kentucky, Lexington, Kentucky, pp. 1-4, 9-12, 15, and 20.

(8)   Gutierrez, M. J., J.R. Edwards, C.P.L. Barkan, B. Wilson, J. Mediavilla, "Advancements in Fastening System Design for North American Concrete

Crossties in Heavy Haul Service," *Proceedings of the 2010 Annual AREMA Conference*, Orlando, FL, August 2010, pp. 5.

(9)   Tekscan®, Inc., "Sensor Model / Map: 5250," Online Reference, URL: http://www.tekscan.com/5250-pressure-sensor. 14 May 2012.

(10)   *Handbook of Railway Vehicle Dynamics,* 2006, CRC Press, Taylor & Francis Group, Boca Raton, Florida, pp. 212.

(11)   Oldknow, K.D., Eadie, D.T., "Top of Rail Friction Control as a Means to Mitigate Lateral Loads Due to Overbalanced Operation of Heavy Axle Load Freight Traffic in Shared High Speed Rail Corridors," *Proceedings of the 2010 Joint Rail Conference,* Urbana, IL, April 2010, pp. 1 and 2.

(12)   Hay, W.W., 1982, *Railroad* Engineering, 2nd ed., John Wiley & Sons, Inc., New York City, New York, Ch. 23, pg.471 and 473.

(13)   Giannakos, K., Loizos, A., "Evaluation of actions on concrete sleepers as design loads – influence of fastenings," *International Journal of Pavement Engineering,* Volume 11, Issue 3, 2010, pp. 209

(14)   Amtrak Engineering, Load Spectra of the Northeast Corridor, Transportation Research Board 90th Annual Meeting, 2011, Washington, D.C.

TABLES

FIGURES